Chapter 20

The ocean and climate change

In this final chapter we turn from the short-term climate variability of ENSO to consider variations with timescales of several decades or more. Small but persistent changes in climate can have a huge impact on the ecosphere (the finely tuned interplay between living matter and its environment). Such changes can occur naturally, as they have done in the past, experienced for example as ice ages and interglacial periods. This century is witnessing the possibility of climate changes through human activity. The last few decades have seen the introduction of the so-called greenhouse gases (CO_2, CH_4 and others) into the atmosphere on an ever increasing scale; this alters the radiation balance and may result in climate changes of magnitudes comparable to those which occurred naturally in the past. Many countries therefore have made research into these longer-term variations a national priority, and oceanographers are asked to quantify the role of the oceans in long-term climate change. However, when oceanographers try to come to grips with longer-term changes in the ocean, they immediately find themselves facing a major problem - the very patchy nature of the observational record. There have been large fluctuations in the number and spatial distribution of observations made over the decades, as shipping routes changed and wars interrupted continuous data collection and research plans. In many cases the technology used changed drastically over time, and data in the same series are not directly comparable. There is considerable risk that changes in observation density and technique may introduce bias, and great care has to be taken in interpreting long time series of ocean data. Nevertheless, as we shall see, there are several incontrovertible examples of changes in the ocean over decades, and some of these lend themselves to preliminary interpretation in terms of large-scale changes in the ocean circulation patterns.

Given the problems with the data, and the rapidly increasing sophistication of ocean numerical models, it is not surprising that climatologists have recently come to rely rather heavily on numerical models to explore the ways in which changes in ocean circulation are likely to occur. These models, and in particular those which couple the ocean with the atmosphere, have generated some valuable ideas about the likely nature of some kinds of longer-term climate variations. Some of these new ideas and their implications are discussed in this chapter.

Using models to extend our limited observational data base into the future is of course risky business, since few of the model predictions can be verified with existing data. Modellers and observationalists are both well aware of the dangers of predicting long-term climate variations in this way. One of the major goals of the international climate research community is therefore directed towards building an observing network that will keep track of climate changes throughout the world ocean, as well as in the atmosphere. How this can be achieved and what is on the drawing board is discussed at the end of this chapter.

The observations

Three major sources are available for inferring changes in ocean circulation over the last hundred years or so. The first is the record of sea surface temperature from merchant ships. Some 150 years ago Captain Matthew Fontaine Maury of the U.S. Navy introduced an

the variations in corrected air and sea temperature track one another quite closely. This gives one some confidence that along major shipping routes averages of each time series over a 10°x10° square for a decade will be reliable to one or two tenths of a °C.

When processed in such a way, i.e. compressed into mean annual values for 10°x10° squares, sea surface temperature is seen to be a function f of space and time defined at constant space and time intervals: SST = f(x,y,t), where x, y represent the longitude and latitude of the centre of the 10°x10° square and t is the year. Several mathematical techniques are available to analyze space and time trends in such data sets. One method regularly used in meteorology and oceanography is a technique known as Empirical Orthogonal Function (EOF) analysis. The method represents the data as a sum of products of functions: f(x,y,t) = Σ F_i(x,y)G_i(t), where the F_i express the data distribution in space and the G_i give the contribution of the respective space distribution to the observed SST field at any given time. Theory shows that an infinite sum of function products can reproduce the observations to any required accuracy and that many such representations of the data are possible. In practical applications the summation is truncated after the first few terms. The strength of EOF analysis lies in the fact that it arranges the contributions of the sum in such a way that the first term ($i = 1$) accounts for more of the variance found in the observations than any other term; the second term ($i = 2$) then accounts for more of the variance found in the difference between the observations and the first term than any of the following terms, and so on. This allows one to extract the dominant spatial and temporal signals with the help of very few function products.

Figures 20.1 - 20.3 show results of an EOF analysis of SST based on a data set similar to COADS but going back to "only" 1900. F_1(x,y), the space function for the first EOF, is shown in Figure 20.1a, while Figure 20.1b shows the corresponding time function G_1(t). The space function is seen to be positive nearly everywhere, and the time function is increasing irregularly with time. The net increase in G_1(t) over the last 80 years is about 0.5°C. The net contribution of the first EOF to SST is given by the product of both functions, which is negative everywhere before 1940 and turns positive from 1975 or so.

This provides fairly convincing evidence that - despite the uncertainties discussed earlier - the sea surface temperature has indeed risen over the present century by about 0.5°C on global average. However, it should be noted that this interpretation relies in part on the particular presentation of the first EOF; a similar analysis for the COADS data set which goes back another fifty years shows the same trend but cooling between 1860 and 1910 (Folland *et al.*, 1984).

As outlined above, the first EOF can be subtracted from SST(x,y,t) and the same analysis applied to the resulting difference, to give the second EOF which describes most of the remaining SST variation. The spatial pattern F_2(x,y) is seen in Figure 20.2a and the corresponding time amplitude G_2(t) in Figure 20.2b. In this case the spatial pattern has a maximum in the eastern Pacific Ocean and is in general closely reminiscent of the ENSO pattern of SST variability seen in Figure 19.6. Furthermore, the time amplitude G_2(t) has maxima at each of the ENSO events. It follows that during ENSO years the product F_2(x,y)G_2(t) has positive values (positive SST anomalies) in the eastern Pacific and negative values (negative SST anomalies) in the western Pacific Ocean, while the reverse is true during anti-ENSO years. In other words, the second EOF can be identified with the ENSO signal in SST discussed in Chapter 19. (EOF analysis also reveals that ENSO events are associated with a *global* warming of the ocean surface; this is seen in the first EOF which shows maxima in G_1(t) during ENSO years.)

such strong spatial and temporal coherence in F_3 and G_3 that this is unlikely. Furthermore, both functions seem to be associated with significant changes in the world's climate. An idea of the magnitude of these effects can be gained from the fact that between 1950 and 1980, the temperature of the southern hemisphere oceans (plus the northern Indian Ocean) increased relative to the rest of the northern hemisphere oceans by about 0.4°C.

Figure 20.3b includes a measure of average rainfall in the Sahel region at the southern edge of the Sahara Desert. There is evidently a fair degree of correlation between the rainfall time series and the third EOF time function G_3(t) of SST. To test whether this correlation is a coincidence or is based in physics, atmospheric numerical models have been run with the SST anomalies of Figure 20.3a superimposed on a mean SST climatology. These generate rainfall anomalies over tropical Africa fairly similar to observation. A plausible explanation is that addition of the SST pattern of Figure 20.3a to climatology shifts the tropical SST maximum northwards. As discussed in the previous two chapters, this tends to move the rainfall maximum north with it. However, the true explanation may be more complex than this, and some time will pass before climatologists will be able to assist the people of the Sahel region to avoid the hardship and suffering which they experience during the present series of droughts.

These examples show that observed changes in SST can be related to observed variations in climate. It is therefore realistic to hope that with our increasing data base we will be able one day to go beyond mere description and come to conclusions about causes and effects.

Sea level measurements and sea level rise

Unlike the merchant ship data for which results are usually averaged over observations from a large number of ships, each tide gauge is an individual instrument. Its reliability over decades depends on the care taken by its operators in preventing fouling and damage, in meticulously recording any shifts in the tide staff fixed to a wall next to the gauge, and in taking accurate surveys every few years to relate the height of the staff to stable bench marks on the shore. 179 stations exist with records of more than 30 years; only 22 of these have records of more than 80 years, and of these only 3 are located outside the northeast Atlantic Ocean. Figure 20.4 shows the locations of sites with records of more than 10 years.

Many of these 179 records have to be rejected for use in long-term climate studies. For example, much of the coast of Japan and western North America is tectonically active, so that all the bench marks to which the tide gauge height has been measured may have shifted by unknown amounts. In fact it is now recognized that *all* tide gauges are subject to slow rises and falls of land level, because the magma beneath the earth's crust is still slowly flowing back towards the regions occupied by thick ice sheets only about 10,000 years ago; however, outside tectonically active areas recent numerical models of this process appear to be successfully capturing the main features of this "postglacial rebound" (Peltier and Tushingham,1991).

Using these data, Gornitz and Lebedeff(1987) found that much of the variations from region to region could be removed if the tide gauge records were corrected for post glacial rebound. After correcting for this effect, Gornitz and Lebedeff found a global mean sea level rise of 1.2±0.3 mm/year. Two more recent estimates of global mean sea level rise in the
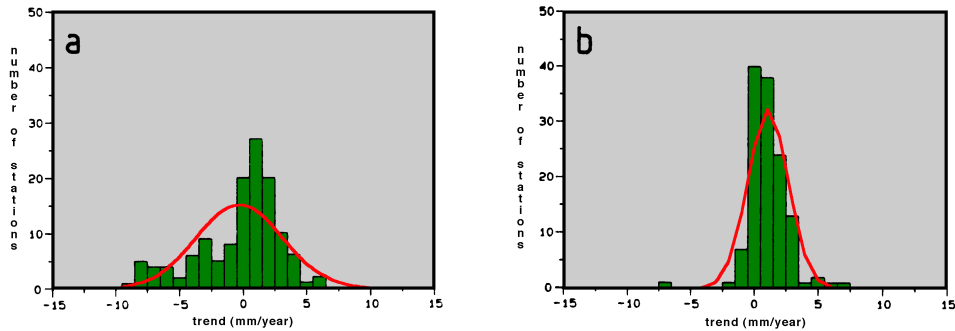
Fig. 20.5. Histograms of sea level trends from all tide gauge records with length of 50 years or longer, (a) before and (b) after correction for postglacial rebound. From Douglas (1991).

Much of this observed sea level rise can be accounted for by thermal expansion of seawater. As seen in Figure 20.1, the ocean has certainly warmed at the surface in the last century, and water expands upon warming. Convergence of Ekman transports and the convective overturn of water after surface cooling results in downward motions in certain parts of the ocean. Both processes provide the principal means by which warmed water is carried below the ocean surface; it is an advective rather than a diffusive process, so its magnitude can be directly estimated from large-scale ocean observations of currents. This makes it somewhat easier to assess thermal expansion rates for a given history of global mean surface temperature rise. The subducted water tends to accumulate in the subtropical gyres. However, Kelvin and Rossby waves tend to redistribute the warming over the rest of the globe; if this process went to completion, and the wind stress field did not change, the increase in depth-integrated steric height would be uniform over the world. This results in a rise in surface steric height (i.e. sea level) that is fairly spatially uniform, though thermal expansion rates are predicted to be somewhat greater in the tropics than near the poles (Figure 20.6). For the global mean SST rise of 0.4°-0.6°C per century inferred from Figure 20.1, the model yields a global mean thermal expansion of 0.8±0.2 mm/year.
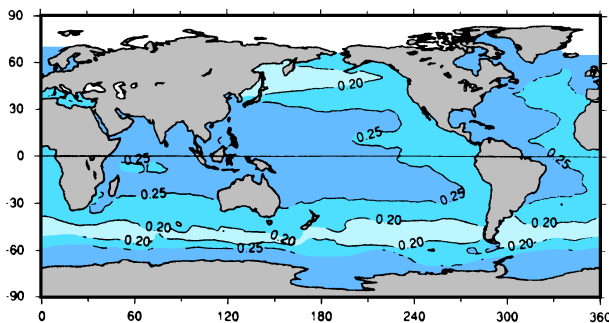

Fig. 20.6. Estimated sea level rise (m) by 2050 caused by thermal expansion, from the model of Church *et al.* (1991), assuming a global averaged temperature increase of 3°C by 2050.

years seen in Figure 20.7 occurs quite close to this mean sea level drop. It is rather reasonable to suppose that the 0.7 m sea level drop might have changed by 0.05 m, or 7%, over the last 50 years due to changes in climate.

Fig. 20.7. Trends of sea level (corrected for postglacial rebound) on the North American east coast, 1930-1980, plotted as a function of latitude. From Douglas (1991).
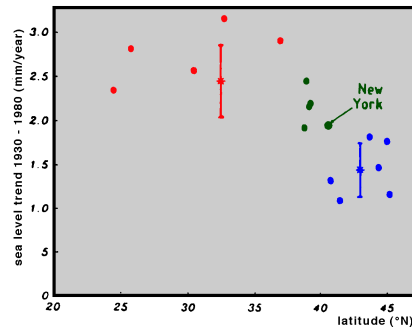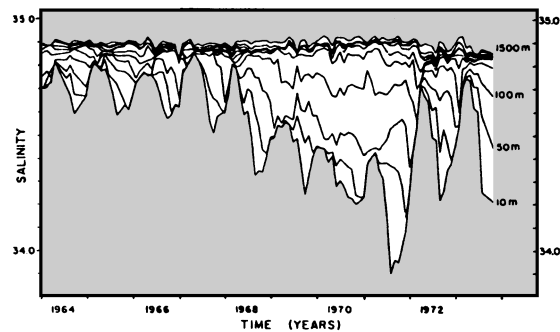

Fig. 20.8. Time series of monthly mean salinities at Ocean Weather Station Bravo, (56°30'N, 51°W), for 1964-1974. From Lazier (1980).

Ocean hydrology

The third source of long-term data for the ocean comes from accurate hydrological observations made by ocean research vessels and Ocean Weather Stations. The latter are vessels that have been stationed at fixed locations for some decades to supplement the land-based meteorological observation network and provide advance warning of weather events approaching the continents. Figure 20.8 shows a time series of monthly average salinity profiles based on data collected daily from Ocean Weather Station Bravo (56°30'N, 51°00'W) near the centre of the Labrador Sea. Freshening in late summer is evident at 10 m each year; in winter, salinity increases due to sea-ice formation. In most winters, a slight freshening can be seen at and below 100 m, bringing winter salinities close together over the top several hundred meters; this is due to convective overturn of the relatively fresh but cold waters above. Maximum mixed layer depths reached to over 1000 m in the winters of 1964-65, 1966-67, 1971-72 and 1972-73. However, from 1967-1971 the surface salinity was significantly lower than in other years, and mixed layers in these winters only penetrated to

appearance is of significant weakening of the density gradients across the Gulf Stream over this period, and hence (through geostrophy) a weakening of the near-surface Gulf Stream itself. However, a time series (Figure 20.10c) of the depth of the 26.5 σ_θ surface at 32°N, 64°W near the maximum depth of this isopycnal surface suggests that the shallowing near this location is not part of a longer-term trend but is associated with a minimum depth of the isopycnal surface in the early 1970s. Much more systematic monitoring of the oceans is required to link these observations with possible climate trends.

These broad-scale changes in the Atlantic subtropical gyre seem to involve changes in isopycnal depths without much clear signal in the water mass structure. Changes in water mass properties can be investigated by monitoring changes of potential temperature for given densities. As an example, Figure 20.11 shows the change in potential temperature on potential density surfaces along 49.5°W. A systematic cooling and therefore freshening is apparent north of 45°N; though it should be noted that this is a near-surface effect (water with $\sigma_\theta < 27.5$ is confined to the top 200 m at these latitudes).
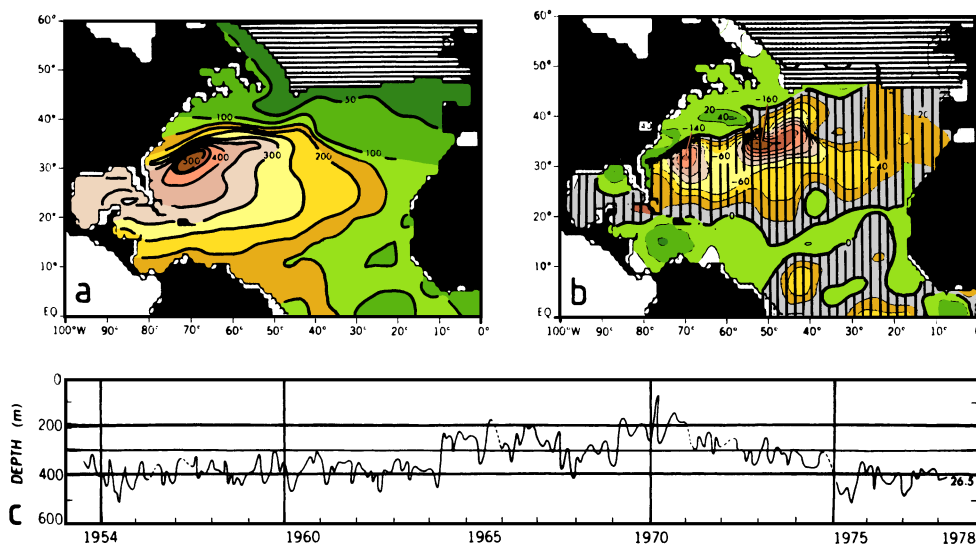

Fig. 20.10. Changes in thermocline depth in the North Atlantic Ocean. (a) Depth (m) of the 26.5 σ_θ surface for 1955-1959; hatching indicates regions where the surface does not exist, (b) depth difference (m) of the 26.5 σ_θ surface 1970-74 minus 1955-59, (c) depth of the 26.5 σ_θ surface at 32°N, 64°W for 1954-1978. Adapted from Levitus (1989).

It would be useful to extend such studies to the Southern Hemisphere, but opportunities for doing so are unfortunately rare. One recent example uses hydrographic sections at 43°S and 28°S in the western South Pacific Ocean taken in 1967 and repeated in 1989-90. Over the 22 years between these sections, there has been a depth-averaged warming at most depths below the surface mixed layer (Bindoff and Church, 1992). As in the case of the Atlantic Ocean, these changes are mostly due to changes in isopycnal depth with rather

have revealed the existence of (at least) two stable steady states. One of these steady states corresponds to the circulation system we observe today, with North Atlantic Deep Water formation and recirculation through all ocean basins. The other steady state does not have North Atlantic Deep Water formation; it shows a very much colder and fresher north Atlantic Ocean and very little Deep Water exchange between the three major oceans. Figure 20.12 shows the SST difference between the two possible steady solutions. Compared to the present situation, the solution without NADW formation shows the north Atlantic Ocean colder by as much as 7°C and the north Pacific Ocean colder by some 2°C. The qualitative resemblance between Figure 20.12 and the third EOF derived from SST data (Figure 20.3a) is striking; however the amplitude of the SST differences of Figure 20.12 is larger than the largest differences associated with the third EOF by a factor of 5. One way of interpreting this is to say that the data support the possibility of an alternative steady state of the oceanic circulation, in the sense that the time function G_3(t) can be seen as an indicator for the speed with which the ocean circulation may be changing from one steady state to the other.
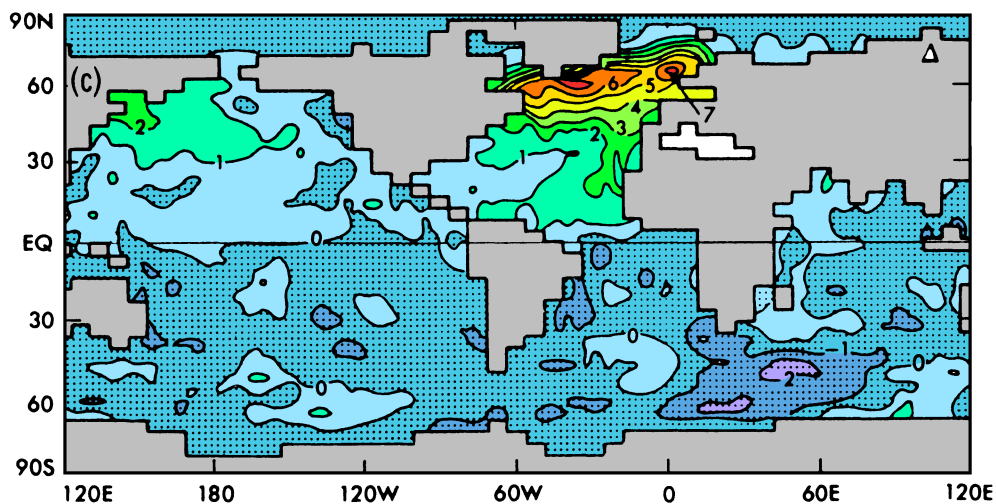

Fig. 20.12. Difference in sea surface temperature, T_1 - T_2 (°C), between two stable steady states of the oceanic circulation found in a coupled ocean/atmosphere model. T_1 is SST in the model with NADW formation, T_2 is SST in the model without NADW formation. From Manabe and Stouffer (1988).

The existence of two steady states may seem to contradict our argument from Chapter 18 that a cold but fresh north Atlantic Ocean will eventually return to its present state by increasing its salinity through water vapour export across Central America. However, if the change in north Atlantic SST is large enough (and a 7°C SST difference is an enormous change) it might be expected to have a major effect on the atmospheric circulation and associated rainfall which might result in a suppression of water vapour export from the Atlantic Ocean. A large shift in the distribution of tropical rainfall was indeed found in the

While the model results and possible scenarios are extremely interesting, they are only indicative of the types of phenomena that may occur in the real coupled ocean-atmosphere system. They give us no indication, for example, whether the fluctuations of the north Atlantic gyre discussed above are associated with some coupled ocean-atmosphere fluctuation or merely a response to random fluctuations in atmospheric forcing; nor do we have the data to know if such phenomena are occurring in most of the other basins. Regional oceanographers and modellers agree that there is a lamentable gap between the comprehensive global coverage of the ocean apparently provided by models and the extraordinarily sparse nature of the data base with which to verify them. We will certainly be living with this problem for some decades. However, oceanographers are devoting considerable efforts to improving the situation. The World Ocean Circulation Experiment (WOCE) introduced in Chapter 2 is one component of the strategy, TOGA (see Chapter 19) another. Out of these efforts will evolve the Global Ocean Observation System (GOOS) as the equivalent of the network of meteorological observations supported by all member countries of the World Meteorological Organization (WMO). Although it will have a very similar function, namely the provision of real-time data for the forecasting of the oceanic circulation, it will have to be based on very different technology. Factors affecting its design are the lack of availability of voluntary observers for many ocean regions and the - in comparison to atmospheric space scales - much smaller scales of oceanic eddies and frontal variability. The increased demand posed by small space scales is partly compensated by the much longer oceanic time scales which allow less frequent sampling than in the atmosphere. Scientists involved in the design of GOOS are actively working on questions of data resolution in space and time required for forecasting the variability of the oceanic circulation.